

# Modeling Of Vegetated Open Channel Flow: A Review

ABDULLAHI, N<sup>1</sup>, BUSARI, A. O.<sup>2</sup>

<sup>1</sup> Department of Civil Engineering, Federal Polytechnic, Bida, Niger State, Nigeria

<sup>2</sup> Department of Civil Engineering, Federal University of Technology, Minna, Niger State, Nigeria

**Abstract-** *The presence of vegetation growth in waterways such as lakes, rivers and canals e. t. c. play an important role from ecological point of view as it can be used to improve water quality and reduce soil erosion by altering the flow magnitude. To understand the hydrodynamics of vegetation, numerous types of synthetic materials were used to simulate vegetation roughness in the past. Through this, numerous model equations were developed to predict the discharge, but the models were found to overestimate the discharge when applied to a natural vegetated channel or constructed one such as flumes. This paper reviews some researches performed on vegetated open channels, which comprises the effects of vegetation characteristics on flow, modeling of vegetative roughness and derivation of vegetal drag coefficient due to submerged and emergent vegetation. Studies based on laboratory, field works, mathematical/analytical and numerical modeling, have been reviewed based on previous approaches by different researchers. The paper concludes with recommendations for future work in order to improve the existing models for predicting vegetated roughness through the use of natural vegetation in combination of both the interactions of submerged, emergent and floating types of vegetation which is less investigated by researchers. For this reason, it remains questionable to precisely determine the optimum value of vegetative roughness for the purpose of vegetated channel design.*

**Indexed Terms-** *open channel flow, modeling, vegetation roughness, submerged, emergent.*

## I. INTRODUCTION

The importance of vegetation growth in waterways cannot be over-stressed for its ecological benefits in improving water quality and reducing soil erosion by altering the flow magnitude. However, vegetation has to be controlled to an acceptable level to enhance the channel performance, as growing of aquatic plants in

channels generally produce large obstructions that offer considerable resistance to water flow, particularly if the vegetation is emergent (Mitchell, 1974).

Several researches indicated that aquatic vegetation in a channel have a negative impact on the design flow rate, conveyance capacity and permissible velocity by reducing their magnitudes up to 97%, 29% and 6% respectively (Guscio, et al. 1965; Gwinn and Ree, 1980). Also, it was reported that both density and distribution of submerged aquatic weeds had a significant impact on the efficiency and equitability of water distribution (El-Samman, 1999). Thus, increasing the density or distribution of vegetation in a channel, it reduces the flow and obstructs water to reach the downstream and consequently the upstream will be subjected to flooding.

In spite of the above disadvantages of vegetation, it was identified that vegetation has the ability to increase bank stability, reduce erosion and turbidity, provide habitat for aquatic and terrestrial wildlife, attenuate floods, present aesthetic properties and filter pollutants (David, 2008). Also, vegetation can be used as a tool in maintaining the shape of rivers as well as preventing coastal erosion, and the breaking down of wave energy (Nepf, 1999; Stoesser et al. 2003).

Hence, the study of flow in vegetated channels is very vital for understanding and managing earth channels, swales, rivers, flood plains, wetlands and any similar aquatic environments through the application of open channel flow principles (McNaughton, 2009).

Considering the pros and cons of vegetation, vegetation can be used in constructing waterways for its aesthetic value in maintaining sound aquatic environments. Besides this, in urban areas where water pollution is very high due to development, the use of swales as conveyance can improve the storm water quality by trapping and settling of sediments as a result

of decrease in flow velocity. In the same vein, the plant roots help in compacting soil particles and decrease the hazard of erosion. And most importantly, the vegetation substrate can trap particulate matter, heavy metals and oils from runoff before entering into natural water bodies (Buckman, 2013).

Moreover, to understand the hydrodynamics of vegetation, several experiments were conducted using a laboratory flume. Materials like plastics, metals, woods, horse-hairs and so forth were used to simulate the vegetation as a cylindrical element with thickness and height. The vegetal resistance (drag) on flow was evaluated based on a force equilibrium model. Applying this concept, (Wu et al. 1999; Lauren, 2007; Sun and Shiono, 2009 and Hassan, 2010) have developed some relationships that linked the flow parameters and vegetation properties under a controlled experimental setting. And to some extent, they were able to validate their computational results using the prototype of their models. However, some scholars have questioned the use of synthetic materials in modeling vegetative roughness which make it even challenging to be universally accepted in the field of hydraulics (Aberle and Järvelä, 2013; Lauren, 2007; O'Hare et al. 2010). Noting on the dynamic changes in roughness between plants of even the same species, the scholars recommended that further validation using actual plants would be needed for their models to be confidently applied in real-life scenarios.

The main purpose of this paper is to review some of the past studies about flow – vegetation interactions that will provide details on various modeling approaches of vegetated channel flow based on the comprehensive literature study. In this way, future challenges on how to enhance the prediction of vegetative roughness and vegetal discharges will be proposed.

## II. CHARACTERISTICS OF AQUATIC VEGETATION

Naturally, there is great variability among aquatic vegetation in terms of density and height of their distribution, which can be observed even among plants of the same species. Considering, the stem of individual plants for example, there are differences in stiffness, buoyancy and the stem geometry. Thus,

different species vary from being completely rigid to highly flexible. In the same line, looking at height of the vegetation canopy (cover), vegetation may be divided into two general classes as emergent and submerged. The emergent aquatic plants grow right from the channel bed and extend above the depth of flow, while submerged vegetation remain underneath the flow depth allowing water to pass over them (Rominger, 2007). Another class of vegetation in this respect is the floating type of vegetation which floats freely on surface of water over a considerable distance especially when its roots does not get anchored to the soil at the bottom of the water body (Lidia, 2002).

## III. EFFECTS OF VEGETATION IN OPEN CHANNEL FLOW

The occurrence of vegetation in water courses has numerous impacts by at least altering the magnitude and direction of flow which will affect the shape of velocity profile, turbulence structures, and sediment transport in an open-channel flow. The vertical velocity profiles were presumed to be logarithmic in a typical open-channel flows without vegetation (Nezu and Nakagawa, 1993; Chow, 1959) as in Figure 1. Conversely, vegetation modifies the velocity profile within and above the canopy by creating some resistance to flow. For example, the velocity profile is generally uniform over the depth when the vegetation is emergent (Stone and Shen, 2002; Tsujimoto and Kitamura, 1990). And for submerged vegetation, the velocity profile was approximately S-shaped as in Figure 2 (Carollo et al. 2002; Ikeda and Kanazawa, 1996; Kouwen et al. 1969; Temple, 1986). Hence, for both situations the flow velocity within the vegetation zone is reduced greatly compared to that in the surface zone.

Similarly, there exists an inflection point close to the vegetation edge of the velocity profile where substantial shear instability and maximum turbulence intensity are observed (Ikeda and Kanazawa, 1996; Nezu and Sanjou, 2008). Thus, the horizontal and vertical turbulent intensities reached maximum just above and below the canopy respectively.

Consequently, the Reynolds shear stress peaks just below the top of the canopy and declines downwards (Nezu and Sanjou, 2008).

In addition, another parameter that needs to be considered in this respect is the vegetal drag coefficient which account for the features of vegetation. The drag is categorized into three including- grain roughness, form roughness, and vegetative roughness. The vegetation drag dominates the other drags as it has the utmost flow resistance that eventually reduces the mean flow in vegetated regions (Nepf, 1999). This means there will be a corresponding increase in both the flow depth and the residence time of sediments due to drag of vegetation. However, with the discoveries above, it was noted that there are discrepancies for the findings of vegetation drag which necessitate for a general formula in determination of drag coefficient (Nguyen, 2012). Accordingly, it becomes apparent that, describing the velocity profile in vegetated channels will continue to be challenging as the flow over submerged vegetation could be divided into two or three layers and this has not been adequately addressed for the case of depth – limited vegetation flow condition (Nguyen, 2012).

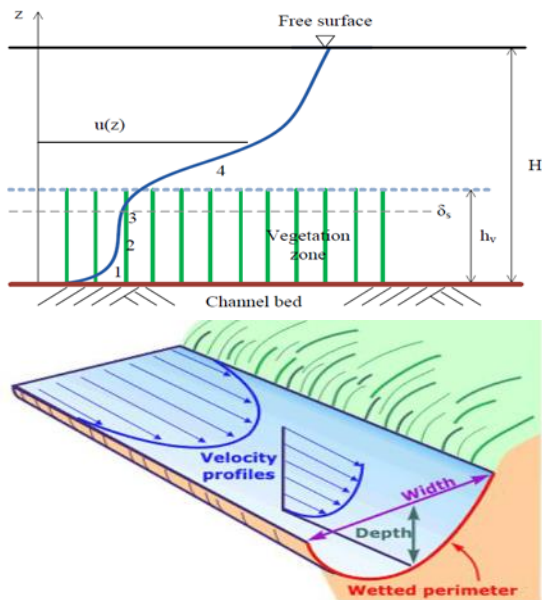


Figure 1; Vertical Velocity Profile of Submerged Vegetation (Baptisetal.2007)

#### IV. MODELING VEGETATIVE ROUGHNESS

As stated earlier, many previous works in deriving vegetative roughness were conducted under controlled conditions using laboratory flume by considering vegetative element as an artificial cylindrical object with diameter and height in order to investigate the

effect of vegetative resistance on flow. Through this lots of equations were developed to relate flow resistance with water depth, velocity, drag coefficient and vegetation density – defined as the frontal area of vegetation per volume (Hamimed, et al. 2013; Hassan, 2010; Li et al., 2014; Sun and Shiono, 2009; Tang, et al. 2014; Xia and Nehal, 2013).

Sun and Shiono, 2009 have investigated experimentally, the flow resistance in a straight compound channel with and without one-line emergent vegetation along the floodplain edge, with simulated rigid vegetation using a constant roughness in which stream-wise velocities and boundary shear stresses were determined. They were able to come up with a formula for friction factors for with and without vegetation cases respectively by using vegetation density and channel geometry based on friction factor method. Even though the formula was developed by simulating only emergent vegetation, it may be used to predict the stage -discharge rating curve in a vegetated channel (Sun &Shiono, 2009).

From the study of Hassan, 2010, an approach for estimating the equivalent Manning coefficient, total flow conveyance, depth average velocity distribution and bed shear stress of trapezoidal channel cross - section with different roughness of flexible vegetation along the wetted perimeter was developed based on a 2D velocity distribution in experimental flume for both submerged and emergent conditions. However, the flow conveyance model was validated in the field and it was found that the model overestimates the discharge especially for vegetation on bed and side banks (Hassan, 2010). This overestimation may be simply because of using synthetic material to represent vegetation roughness during his experiments.

The effect of emergent bending riparian zone vegetation on the flow was studied by Xia and Nehal, 2013 using simulated plastics of *Acorus calamus* plant. They found out that the roughness of the plant has a significant influence on resistance, velocity distribution and turbulence intensity. For example, Manning coefficient increases greatly with increase in vegetation densities making the position of maximum velocity to be further away from the bed and the turbulence intensity was pronounced especially at the middle height of the stem. However, their study

centers on only one plant without considering other forms of vegetation along riparian zones so as to model the roughness by combining different vegetation types.

Similarly, Li et al. 2014 examined the flow structure through artificial submerged flexible vegetation experimentally with the aid of 3D Acoustic Doppler Velocimeter (ADV) in an open -channel flume. They were able to derive relationships to show the variations of velocity profile, Manning coefficient and flow discharge ratio with vegetation density based on their observed data. And there was positive correlation among these variables especially the Manning coefficient was highly correlated to vegetation density and inflow rate. This was supported by the work of Hamimed et al., 2013, even though in this case, emergent vegetation was used to explore the impact of vegetation density on flow. But Hamimed et al. 2013 recommended that other tests should be carried out in natural channels to confirm the validity of their results.

Furthermore, it was illustrated by the study of Tang et al. 2014 that the vegetation drag coefficient can be obtained in three different forms that includes the drag coefficient for an isolated cylinder, the bulk drag coefficient of an array of cylinders and the vertically distributed or local drag coefficient which were used to represent the vegetation drag force. From this, three model equations were developed for the respective

drag coefficients in order to predict the velocity distributions. These models successfully predicted the velocity distribution, but the model with the bulk drag coefficient, estimated larger velocity values compared to the actual measurement. To improve this situation, there is need to incorporate the bed friction effect during the modeling process with particular attention in selecting suitable depth averaged velocity inside the plant layer.

In order to enhance the practical applicability of predicting discharges in vegetated water bodies some few researchers like Helmio, 2005; Wilson, 2006; Chen, et al. 2009; O’Hare et al. 2010; Afzalimehr et al. 2011, Noor et al. 2011 and Huthof et al 2013 have used natural vegetation in channels and/or rivers using the concepts above to develop the flow resistance equations due to vegetation (see Table 1). However, these were not universally accepted because of the fact that their models need to be tested in different rivers of various geometries (Helmio, 2005) while in some cases majority of the field studies were made at or near the base flow and could not account in any change in the roughness character of the plants with increase in discharge (O’Hare et al., 2010). Besides, as aquatic vegetation is highly heterogeneous, there is lack of combining the various vegetation types for optimum roughness determination that will assist in economic design of drainages bearing in mind on the pros and cons of vegetation in a watercourse.

Table 1; Studies Using Natural Vegetation by Various Authors

Author (s)	Findings	Remarks
Helmio,2005	Developed 1D flow model, which was applied to a river with partially vegetated flood plains and found that the estimated discharges and water depths had a good correlation when compared to the observed.	There is need for the model to be tested in different sizes and shapes of rivers, in order to improve it.
Chen et al. 2009	Demonstrated that the resistance coefficient due to vegetation is highly related to the Froude number exponentially.	Used a constant plant height of 10cm throughout the experiment under submerged condition only.

Afzalimehr, <i>etal.</i> 2011	Investigated the turbulence characteristics in channel with dense vegetation, and pointed out that there is a turning point along the velocity profile that coincides with the maximum turbulence intensity just above the vegetation cover.	Considers only two aspect ratios under submerged, this will not give adequate room to vary the flow.
Noor, <i>etal.</i> 2011	Examine the hydraulic characteristic of swales based on estimating the Manning’s resistance, and they found that the Manning decreases with increase in flow depth for a constant vegetative height	Further investigation of swale grass is required.
Huthoff, 2013	Uses a simple hydraulic resistance model that give slight discrepancies in estimating flow in vegetated waterways	Vegetation roughness change

4.1 EXPERIMENTAL CONDITION OF PREVIOUS STUDIES

Table 2 below gives a brief summary on the experimental conditions of past studies with different ways of arranging the vegetated element in form of ford shape with different diameters. It will be noted from Table 2 that various flow and vegetation conditions have been employed by different researchers. For instance, while smooth sidewalls were used in all studies using rectangular channel, the

channel bed involved was either smooth (as in the case of Kothyari et al. 2009; Tanino and Nepf 2008; Nguyen, 2012) or sand-covered (like Ferreira et al. 2009; Ishikawa et al. 2000; James et al. 2004; Liu et al. 2008). Ishikawa et al. (2000) and Kothyari et al. (2009) used strain gauge to measure the drag force directly, while the others estimated the drag from the energy slope of uniform or non-uniform flow conditions.

Table 2; Summary of Experimental Condition of past Studies

Author	Flow conditions				
	Surface Area (m <sup>2</sup> )	Density $\tau$ (m-1)	Stem diameter d (mm)	Arrangement	
Ishikawa <i>et al.</i> 2000	15 x 0.3	0.00314- 0.0126	4 & 6.4	Staggered	Uniform
James <i>et al.</i> 2004	--	0.0035 - 0.0314	5	Staggered	Uniform
Liu <i>et al.</i> 2008	3 x 0.3	0.0031- 0.0160	6.35	Staggered & linear	Uniform
Tanino and Nepf, 2008	6.7 x0.203	0.0910	6.4	Random	Non – uniform
Ferreira <i>et al.</i> 2009	3.1 x0.409	0.022 - 0.038	11	Random	Non – uniform

Kothyari <i>et al.</i> 2009	1.8 x 0.5	0.0022 - 0.0885	10	Staggered	Non – uniform
Nguyen, 2012	9.6 x 0.3	0.0043- 0.119	3.2, 6.6 & 8.3	Staggered	Non – uniform

Table 3; Technical details of data using Rigid Vegetation type

Author(s)	Number of Experiments	Dimension flume (LxWxH)	Vegetation type	Measured velocity
Einstein & Banks (1950)	19	L = 5.18 m W = 0.30 m H = 0.46 m	Pins	Calculated from the measured discharge and water level
Shimizu & Tsujimoto (1994)	12	Not mentioned	Plastic cylinders	Micro-propeller Current meter
Stone & Shen (2002)	136	L = 12 m W = 0.45 m H = 0.61 m	Wooden, circular dowels of uniform size	Marsh Mc Birney model
Poggi et al. (2004)	5	L = 18 m W = 0.90 m H = 1.0 m	Stainless steel cylinders	A two-component laser Doppler anemometry (LDA)
Murphy et al. (2007)	27	L = 24 m W = 0.38 m H = 0.47 m	Wooden cylinders	(3-D) acoustic Doppler velocity meters (ADV)

Table 4; Technical details of data using Flexible Vegetation type

Author(s)	Number of Experiments	Dimension flume (LxWxH)	Vegetation type	Measured velocity
Tsujimoto et al. (1991)	6	L = 12m W = 0.40 m	Plastic strips	Micro-propeller Current meter
Freeman et al. (2002)	77	Large flume: L = 152.4 m W = 2.44 m H = 1.82 m	Real (flexible) plants of 21 different species	Marsh Mc Birney Model 201b portable water current meter.
Rowinski et al. (2002)	8	L = 16 m W = 0,58 m H = 0.60 m	Flexible elements	Electromagnetic liquid velocity meter
Carollo et al. (2005)	80	L = 14.4 m W = 0.60 m H = 0.60 m	Grass	Calculated from the measured discharge and water level

Table 5; Technical Details of Existing Dataset

Author(s)	Number of Experiments	Dimensions flume (LxWxH)	Vegetation type	Measured velocity
Dunn et al. (1996)	5	L = 19,50 m W = 0,91 m H = 0,61 m	Cylindrical wooden dowels	Acoustic Doppler Velocimeter
Meijer (1998b)	48	L = 100 m W = 3 m H = 3 m	Vertical steel bars	Acoustic Doppler Velocimeter
Ree and Crow (1977)	14	L = 183 m W = 6,1 m H = 0,91 m	Natural flexible vegetation	2-foot Parshal flume and with the weir
Murota et al. (1984)	8	L = 20 m W = 0,5 m H = 0,35 m	Flexible standing elements of synthetic resin	Constant-temperature anemometer with a dual sensor hot film probe
Tsujimoto et al. (1993)	12	Not mentioned	Flexible nylon cylinders	Electromagnetic current meter
Ikeda & Kanazawa (1996)	7	L = 15 m W = 0,4 m	Nylon filaments	Two-component laser Doppler Velocimeter
Meijer (1998a)	7	L = 100 m W = 3 m H = 3 m	Natural reed	
Järvelä (2003)	12	L = 50 m W = 1,1 m H = 1,3 m	Wheat and sedges	3D acoustic Doppler Velocimeter

A short description of the experiments mentioned in Table 3, 4 and 5 as given above. First the aim of the experiments (and some specialties) is given. Second a table with some technical details is given. Finally, special attention is given to the way the drag coefficient and slope are determined. Einstein and Banks (1950) conducted flume experiments to determine the resistance of different types of obstacles opposing the flow of water through an open channel. Shimizu and Tsujimoto (1994) These authors derived flume experiments to validate their numerically analyzed k-d turbulence model. Stone and Shen (2002) conducted experiments under emergent and submerged conditions to determine the hydraulic resistance characteristics of a channel with vegetation. Poggi et al. (2004) conducted flume experiments to examine the inter-connection between

vegetation density and key flow statics within and just above the vegetation, as needed for quantifying momentum and scalar transport. Murphy et al. (2007)

described flume experiments with rigid model vegetation to study the structure of coherent vortices and vertical transport in shallow vegetated shear flows. Information is also extracted from the following related articles; Ghisalberti and Nepf (2004) and Ghisalberti and Nepf (2006).

Tsujimoto et al. (1991) measured the turbulence characteristics of flexible vegetation under emergent and submerged conditions in a laboratory flume. The deflected plant height was measured under uniform flow conditions by eyes and by means of video-film analysis for a special case. Freeman et al. (2002) investigated the effect of natural vegetation, particularly ground cover plants, small trees, and shrubs, on flow resistance under emergent and submerged conditions. Thirteen different plant types in groups of uniform sized plants and groups of mixed plants with varying plant density, sizes and shapes were used to measure in situ flow resistance and drag force. Freeman et al. (2002) measured the drag force

instead of the drag coefficient. Therefore, it is investigated if the drag coefficient can be calculated from the given drag force. Freeman et al. (2002) gave values of the drag force for certain velocities for four different plant species. So, it was not possible to calculate the drag coefficient for the other species. The blockage area was given for 27 plant species. For two of the four plant species used to measure the drag force, information about the blockage area was lacking. However, information about the width of the plant and the erected plant height was given. Assuming uniform width of the plant over the height and multiplying with the height, results in the blockage area. Unfortunately, the deflected plant height was not given by Freeman et al. (2002). Because they used flexible plants with side-branches and foliage, that parameter became important. Due to bending of the vegetation the blockage area becomes smaller with increasing velocity, and therefore the drag coefficient decreases. Rowinski et al. (2002) Submerged vegetation was simulated in a flume, with small cylindrical little stems of elliptical cross-sections to study the problem of the proper evolution of the vertical velocity distributions in vegetated channels. Carollo et al. (2005) collected experimental data from a bed covered by grass like vegetation to analyze flow resistance. Carollo et al. (2005) used very flexible vegetation with deflected plant heights of half the erected plant heights. The flexible vegetation changes with velocity so the drag force is very important. However, Carollo et al. (2005) did not mention a drag coefficient at all. As mentioned before, drag coefficient of 1 are used for rigid vegetation. For very flexible vegetation it is questioned if a drag coefficient of 1 is realistic. Nevertheless, a drag coefficient of 1 is assumed.

#### 4.2 ANALYTICAL MODEL APPROACH

In order to predict the vegetation deflection height, the large- deflection cantilever beam theory is usually used. In the theory, the flow influenced by the vegetated layer is considered. In open channel flow, the vegetated bed contributes significantly to the drag and friction factors, hence to the overall flow behaviour (as shown in Fig. 2). The deflected flexible plant's resistance of the bottom vegetated section is considered by taking into account plant bending. The deflection height of the flexible vegetation is obtained when bending occurs; and, according to Chen (2010),

if the cantilever beam- alike material remains linearly elastic, the relationship between the bending moment and beam deformation can be described as follows

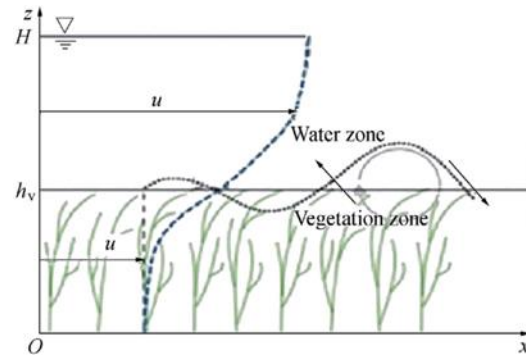


Figure 2; Sketch of open channel flow with submerged vegetation.

$$\frac{d^2/dz^2}{(1+dx/dz)^{3/2}} = \frac{M(z)}{EI} \quad (1)$$

where x and z are coordinates, with x being along the stream wise direction and z being parallel to the original beam; M is the bending moment (N.m); E is the modulus of elasticity of the material (N/m<sup>2</sup>); and I is the moment of inertia of the cross-sectional area of the beam regarding the axis of bending (m<sup>4</sup>). Considering a small element from the bending beam and  $\theta$  as the angle of deflection, with  $\tan \theta = dx = dz$ , the following relationship can be obtained from integration

$$\sin \theta = \int_0^z \frac{M(z)}{EI} dz \quad (2)$$

The curve length of the beam can then be calculated

$$s(h_v) = \int_0^z \sqrt{1 + \left(\frac{dx}{dz}\right)^2} dz \quad (3)$$

where S is the curve length of the bending beam (m), and  $h_v$  is the projective height of vegetation after bending (m). Assigning P as the total load (N) uniformly distributed in flowing water over the bending vegetation and normal to the z- axis, the bending moment can be expressed as

$$M(z) = \frac{P(h_v - z)^2}{2h_v} \quad (4)$$

Substituting Eq. (4) into Eq. (2) results in

$$\sin \theta = \frac{P}{2EI} \left( \frac{z^3}{3h_v} - z^2 + zh_v \right) \quad (5)$$

From Eqs. (3) and (5), one can further deduce

$$\frac{dx}{dz} = \frac{\sin \theta}{\cos \theta} = \frac{[P/(2EI)] [z^3/(3h_v) - z^2 + zh_v]}{\sqrt{1 - [P/(2EI)]^2 [z^3/(3h_v) - z^2 + zh_v]^2}} \quad (6)$$

Considering force balance between the Reynolds shear stress, gravitational component, and resistance force by vegetation, the momentum equation can be written as (Huai et al., 2013)

$$\frac{\partial r}{\partial z} + pgi - \frac{\partial F_x}{\partial z} = 0 \quad (7)$$

where  $\tau$  is the Reynolds shear stress ( $N/m^2$ ),  $\rho$  is the water density ( $kg/m^3$ ),  $g$  is the gravitational acceleration ( $m/s^2$ ),  $i$  is the bed slope, and  $F_x$  is the resultant force per unit area along the x-axis ( $N/m^2$ ). In the vegetated zone, the Reynolds shear stress can be described as

$$r = pghi \exp [\alpha(z - h_v)] \quad (8)$$

Where  $\alpha$  is a constant; and  $h$  is the water depth above the vegetation top (m), with  $h = H - h_v$ . Considering a small element of flexible vegetation in Fig. 2, theoretically there are two types of forces acting on it: the drag force  $F_D$ , normal to the plant stem ( $N/m^2$ ); and the friction force  $F_f$ , along the plant ( $N/m^2$ ). These forces could be calculated by the following approach proposed by Bootle (1971):

$$dF_D = \frac{1}{2} m C_D p (u \cos \theta)^2 A_f = \frac{1}{2} m C_D p (u \cos \theta)^2 D ds \quad (9)$$

$$dF_f = \frac{1}{2} m C_f p (u \cos \theta)^2 A_s = \frac{1}{2} m C_f p (u \cos \theta)^2 C_p ds \quad (10)$$

where  $m$  is the vegetation density ( $m^2$ );  $A_f$  is the frontal area of the element ( $m^2$ );  $A_s$  is the surface area of the element ( $m^2$ );  $D$  is the frontal-projected width of the stem (m), equal to the stem diameter; and  $C_p$  is the perimeter of the stem cross section (m), and  $C_p = \alpha D$ . For circular cylinders,  $d_s$  can be described as follows:

$$ds = \frac{dz}{\cos \theta} \quad (11)$$

Following Newton's Third Law, the resultant force component  $dF_x$  can be described as

$$dF_x = dF_D \cos \theta + dF_f \sin \theta \quad (12)$$

To find the resultant force of vegetation in a horizontal direction, Eqs. (5) and (9)-(11) can be used in Eq. (12), creating the following formula:

$$\frac{\partial^2 F_x}{\partial z^2} = \frac{1}{2} m p u^2 \left\{ C_d D \left[ 1 - \left( \frac{p g i H}{2 m E I} \right)^2 \left( \frac{z^3}{3 h_v} - z^2 + z h_v + C_r C_p \frac{\{ p g i H / (2 m E I) [z^3 / (3 h_v) - z^2 + z h_v] \}^3}{\sqrt{p g i H / (2 m E I) [z^3 / (3 h_v) - z^2 + z h_v]^2}} \right) \right] \right\} \quad (13)$$

where  $H$  is the total flow depth (m). By substituting Eqs. (8) and (13) into Eq. (7), the vertical velocity distribution in the vegetation layer can be computed as (Huai et al., 2013)

$$u = \sqrt{\frac{2 g i \{ \alpha h \exp [\alpha(z - h_v)] + 1 \}}{m D \left\{ C_D \left[ 1 - \left( \frac{p g i H}{2 m E I} \right)^2 \left( \frac{z^3}{3 h_v} - z^2 + z h_v \right)^2 \right] + n C_r \left( \frac{p g i H}{2 m E I} \right)^2 \left( \frac{z^3}{3 h_v} - z^2 + z h_v \right)^3 \right\} / \sqrt{1 - \left( \frac{p g i H}{2 m E I} \right)^2 \left( \frac{z^3}{3 h_v} - z^2 + z h_v \right)^2}} \quad (14)$$

At the top of the vegetation, where  $z = h_v$ , the flow velocity can be obtained as

$$u = \sqrt{\frac{2 g i (\alpha h + 2)}{m D \left\{ C_D \left[ 1 - \left( \frac{p g i H h_v^2}{6 m E I} \right)^2 \right] + n C_r \left[ \frac{p g i H h_v^2}{6 m E I} \right]^3 / \sqrt{1 - \left( \frac{p g i H h_v^2}{6 m E I} \right)^2}} \right\}} \quad (15)$$

The flow velocity in the free-water layer could also be expressed by the log-law as (Huai et al., 2009; Liu et al., 2012)

$$\frac{u}{u^*} = \frac{h}{h - h_v} \frac{1}{k} \ln \frac{z}{h_v} + \frac{u_v}{u^*} \quad (16)$$

where  $u_v$  is the velocity averaged over the vegetated layer (m/s); and  $u^*$  represents the shear velocity at the top of the vegetation, with  $u^* = \sqrt{g(h - h_v)i}$ .

### 4.3 MATHEMATICAL MODEL APPROACH

The mathematical model of a turbulent flow consists of the Reynolds-Averaged Navier-Stokes (RANS) equations coupled with the k-ε turbulence model. Each

primitive flow variable ( $u, v, w, p$ ) is decomposed to an averaged-in-time part and a fluctuation term., i.e.,

$$u = \bar{u} + u', v = \bar{v} + v', w = \bar{w} + w', p = \bar{p} + p' \quad (17)$$

The use of mean values (in time) in the mass and momentum conservation equations leads to the Reynolds-Averaged Navier-Stokes (RANS) equations:

$$\frac{\partial \bar{u}}{\partial x} + \frac{\partial \bar{v}}{\partial x} + \frac{\partial \bar{w}}{\partial z} = 0 \quad (18)$$

$$\rho \left[ \frac{\partial \bar{u}}{\partial t} + \bar{u} \frac{\partial \bar{u}}{\partial x} + \bar{v} \frac{\partial \bar{u}}{\partial y} + \bar{w} \frac{\partial \bar{u}}{\partial z} \right] = -\frac{\partial \bar{p}}{\partial x} + \rho g_x + \mu \left[ \frac{\partial^2 \bar{u}}{\partial x^2} + \frac{\partial^2 \bar{u}}{\partial y^2} + \frac{\partial^2 \bar{u}}{\partial z^2} \right] - \rho \left[ \frac{\partial \bar{u}^2}{\partial x} + \frac{\partial \bar{u}v}{\partial y} + \frac{\partial \bar{u}w}{\partial z} \right] \quad (19 a)$$

$$\rho \left[ \frac{\partial \bar{v}}{\partial t} + \bar{u} \frac{\partial \bar{v}}{\partial x} + \bar{v} \frac{\partial \bar{v}}{\partial y} + \bar{w} \frac{\partial \bar{v}}{\partial z} \right] = -\frac{\partial \bar{p}}{\partial y} + \rho g_y + \mu \left[ \frac{\partial^2 \bar{v}}{\partial x^2} + \frac{\partial^2 \bar{v}}{\partial y^2} + \frac{\partial^2 \bar{v}}{\partial z^2} \right] - \rho \left[ \frac{\partial \bar{v}u}{\partial x} + \frac{\partial \bar{v}^2}{\partial y} + \frac{\partial \bar{v}w}{\partial z} \right] \quad (19 b)$$

$$\rho \left[ \frac{\partial \bar{w}}{\partial t} + \bar{u} \frac{\partial \bar{w}}{\partial x} + \bar{v} \frac{\partial \bar{w}}{\partial y} + \bar{w} \frac{\partial \bar{w}}{\partial z} \right] = -\frac{\partial \bar{p}}{\partial z} + \rho g_z + \mu \left[ \frac{\partial^2 \bar{w}}{\partial x^2} + \frac{\partial^2 \bar{w}}{\partial y^2} + \frac{\partial^2 \bar{w}}{\partial z^2} \right] - \rho \left[ \frac{\partial \bar{w}u}{\partial x} + \frac{\partial \bar{w}v}{\partial y} + \frac{\partial \bar{w}^2}{\partial z} \right] \quad (19 c)$$

Most of engineering work is based on Boussinesq's hypothesis which is a turbulence closure model that relates the Reynolds stresses (turbulent stresses) with the mean velocity field. For incompressible flow, the 3-D formulation of the Boussinesq's hypothesis is written in indicial notation as:

$$-\overline{u'_i u'_j} = \frac{2}{3} k \delta_{ij} - \nu_T \left( \frac{\partial \bar{u}_i}{\partial x_j} + \frac{\partial \bar{u}_j}{\partial x_i} \right) \quad (20)$$

where  $\nu_T$  is a scalar quantity called kinematic turbulent viscosity or kinematic eddy viscosity and  $k$  is the mean turbulence kinetic energy:

$$k = \frac{1}{2} (\overline{u'^2} + \overline{v'^2} + \overline{w'^2}) = \frac{1}{2} \overline{u'_i u'_i} \quad (21)$$

Equation (4) can be rewritten in the form:

$$R = -2\nu_2 S \quad (22)$$

$\mathbf{I}$  and  $\mathbf{1}$  is the unit tensor. The tensor  $\mathbf{S}$  is the symmetric part of the mean velocity gradient tensor and  $\mathbf{R}$  is an anisotropic tensor defined above.

The calculation of the turbulent viscosity at each point of the flow field is accomplished using the k-ε model. The k-ε model is a two differential equation model where the kinematic eddy viscosity is calculated by:

$$\nu_T = C_\mu \frac{k^2}{\epsilon} \quad (23)$$

Here  $C_\mu$  is a dimensionless quantity. The turbulence kinetic energy per unit,  $k$ , and the rate of turbulence dissipation per unit mass,  $\epsilon$ , are calculated by concurrently solving two transport equations [18]:

$$\frac{\partial k}{\partial t} + \bar{u}_i \frac{\partial k}{\partial x_i} = -\tau_{ij} \frac{\partial \bar{u}_i}{\partial x_j} - \epsilon + \frac{\partial k}{\partial x_i} \left[ \frac{\nu_T}{\sigma_k} + \frac{\partial k}{\partial x_i} \right] + \nu \nabla^2 k \quad (24)$$

$$\frac{\partial \epsilon}{\partial t} + \bar{u}_i \frac{\partial \epsilon}{\partial x_i} = C_{\epsilon 1} \frac{\epsilon}{k} \tau_{ij} \frac{\partial \bar{u}_i}{\partial x_j} - C_{\epsilon 2} \frac{\epsilon^2}{k} + \frac{\partial}{\partial x_i} \left( \frac{\nu_T}{\sigma_\epsilon} + \frac{\partial \epsilon}{\partial x_i} \right) + \nu \nabla^2 \epsilon \quad (25)$$

The standard values of the constants that appear in Equations (23)– (25) are:  $C_\mu = 0.09$ ,

$C_{\epsilon 1} = 1.44$ ,  $C_{\epsilon 2} = 1.92$ ,  $\sigma_k = 1.0$ ,  $\sigma_\epsilon = 1.3$ . Variations of these values appear in the literature.

#### 4.4 NUMERICAL MODEL APPROACH

The k-ε model, is the most commonly used two equation model in engineering and has proved to be a reliable tool in a wide variety of problems in hydraulic and environmental engineering (Rodi 1984). Therefore, it is one of the numerical closure schemes usually selected for various study. The k-ε model has received more attention in the last few years, especially in the mechanical engineering community (Wilcox 1988); it is used herein to provide numerical comparisons. Following the common practice in turbulence closure schemes, it is assumed that the total averaged vertical turbulent transport of longitudinal momentum, in the presence of vegetation, can be modeled using an eddy viscosity approach. This assumption was validated by experimental observations on the relationship between the averaged velocity gradient  $\langle u'_i u'_j \rangle$  and in a laboratory flume with simulated non emergent vegetation (Dunn et al. 1996); it provides good agreement with measurements in the model.

Scheme I:  $\frac{\partial}{\partial x_i} \langle u_i \rangle = 0$  (1a)

Scheme II:  $\frac{\partial}{\partial x_i} \langle \bar{u} \rangle = 0$  (1b)

For momentum conservation, Scheme I yield

$$\frac{\partial \langle u_i \rangle}{\partial t} + \langle u_i \rangle \frac{\partial \langle u_i \rangle}{\partial x_i} + \frac{\partial}{\partial x_j} \langle u_i'' u_j'' \rangle = -\frac{1}{\rho} \frac{\partial \langle p \rangle}{\partial x_i} - \frac{1}{\rho} \langle \frac{\partial p''}{\partial x_i} \rangle + g_i + \nu \nabla^2 \langle u_i \rangle + \nu \langle \nabla^2 u_i'' \rangle$$
 (2)

where  $g_i$  = the component of the gravity vector along the  $i$ -axis;  $\rho$  and  $\nu$  = the fluid density and kinematic viscosity, respectively;  $\nabla^2$  = the Laplacian operator in space; and  $t$  = time

The averaged momentum conservation law under Scheme II is

$$\frac{\partial \langle \bar{u}_i \rangle}{\partial t} + \langle \bar{u}_i \rangle \frac{\partial \langle \bar{u}_i \rangle}{\partial x_i} + \frac{\partial}{\partial x_j} \langle \bar{u}_i'' \bar{u}_j'' \rangle + \frac{\partial}{\partial x_j} \langle \bar{u}_i'' \bar{u}_j'' \rangle = -\frac{1}{\rho} \frac{\partial \langle \bar{p} \rangle}{\partial x_i} - \frac{1}{\rho} \langle \frac{\partial \bar{p}''}{\partial x_i} \rangle + g_i + \nu \nabla^2 \langle \bar{u}_i \rangle + \nu \langle \nabla^2 \bar{u}_i'' \rangle$$
 (3)

The second term on the right-hand side of (2) and (3) represents the drag force, which is parameterized in fluid mechanics using a drag coefficient,  $C_D$ , as  $1 / \rho \langle \partial p'' / \partial x_i \rangle = C_D / 2a \langle u_i \rangle^2$ , where  $a$  = a measure of the density (the ratio between the sum of the differential frontal areas of the obstacles divided by the differential volume of fluid) and has dimensions of  $L^{-1}$ .

The 1D momentum equation for flow through obstacles accounts for a Reynolds stress, due to the usual turbulent momentum transfer,  $\overline{u_i' u_j'}$  and for stresses that arise due to spatial variations of the mean flow field,  $\overline{u_i'' u_j''}$ . The total resulting stress becomes:

$$\langle u_i'' u_j'' \rangle = \langle \bar{u}_i'' \bar{u}_j'' \rangle + \langle \bar{u}_i'' \bar{u}_j'' \rangle$$
 (4)

From a mathematical/physical point of view, it is clear that the simple addition of drag-related body forces in the momentum equation is incorrect, since the dispersive fluxes are not included

• Energy (Second-Order Moment) Equations

The total kinetic energy in Scheme I yields

$$\frac{1}{2} \langle u_i u_i \rangle = \frac{1}{2} \langle u_i \rangle \langle u_i \rangle + \frac{1}{2} \langle u_i'' u_i'' \rangle$$
 (5)

The budget of turbulent kinetic energy in this scheme gives (Raupach and Shaw 1982)

$$\left( \frac{\partial}{\partial t} + \langle u_i \rangle \frac{\partial}{\partial x_i} \right) \frac{\langle u_i'' u_j'' \rangle}{2} = -\langle u_i'' u_j'' \rangle \frac{\partial \langle u_i \rangle}{\partial x_i} - \frac{\partial}{\partial x_i} \left( \frac{\langle u_i'' u_i'' u_j'' \rangle}{2} + \frac{\langle p'' u_i'' \rangle}{\rho} \right) + \nu \langle u_i'' \nabla^2 u_i'' \rangle + \langle \frac{\partial p''}{\partial x_i} \rangle$$
 (6)

The fourth term in (6) accounts for the conversion of both mean and large-scale turbulent kinetic energy to smaller scale turbulent kinetic energy; the latter is sometimes referred to as ‘‘short-circuited cascade’’ (Raupach and Thom 1981). The wake-generated turbulent kinetic energy has a scale proportional to the dimensions of the elements in the canopy, i.e., much smaller than the typical length scales of shear-generated eddies (Raupach and Thom 1981; Raupach and Shaw 1982).

Under averaging Scheme II, the total kinetic energy yields

$$\frac{1}{2} \langle \bar{u}_i \bar{u}_i \rangle = \frac{1}{2} \langle \bar{u}_i \bar{u}_i \rangle + \frac{1}{2} \langle \bar{u}_i'' \bar{u}_i'' \rangle = \frac{1}{2} \langle \bar{u}_i \bar{u}_i \rangle + \frac{1}{2} \langle \bar{u}_i'' \bar{u}_i'' \rangle$$
 (7)

Budgets for each of the last two terms on the right in (7) are readily obtained (Raupach and Shaw 1982)

$$\left( \frac{\partial}{\partial t} + \langle \bar{u}_i \rangle \frac{\partial}{\partial x_i} \right) \frac{\langle \bar{u}_i \bar{u}_i \rangle}{2} = -\langle \bar{u}_i \bar{u}_i \rangle \frac{\partial \langle \bar{u}_i \rangle}{\partial x_i} - \frac{\partial}{\partial x_j} \left[ \frac{\langle \bar{u}_i'' \bar{u}_i'' \rangle}{2} + \frac{\langle \bar{u}_i'' \bar{u}_i'' \bar{u}_j'' \rangle}{2} \right] + \nu \langle \bar{u}_i'' \nabla^2 \bar{u}_i'' \rangle - \langle \bar{u}_i'' \bar{u}_i'' \rangle \frac{\partial \langle \bar{u}_i'' \rangle}{\partial x_j}$$
 (8)

And

$$\left( \frac{\partial}{\partial t} + \langle \bar{u}_i \rangle \frac{\partial}{\partial x_i} \right) \frac{\langle \bar{u}_i'' \bar{u}_i'' \rangle}{2} = -\langle \bar{u}_i'' \bar{u}_i'' \rangle \frac{\partial \langle \bar{u}_j \rangle}{\partial x_i} + \langle \bar{u}_i'' \bar{u}_i'' \rangle \frac{\partial \langle \bar{u}_j \rangle}{\partial x_i} - \frac{\partial}{\partial x_j}$$

$$\left[ \frac{\langle \bar{u}_i'' \bar{u}_i'' \bar{u}_j'' \rangle}{2} + \frac{\langle \bar{u}_i'' \bar{u}_i'' \bar{u}_j'' \rangle}{2} \frac{\langle \bar{p}'' \bar{u}_j'' \rangle}{p} \right] + \nu \langle \bar{u}_i'' \nabla^2 \bar{u}_i'' \rangle + \frac{1}{p} \langle \bar{u}_i \rangle \langle \frac{\partial p''}{\partial x_i} \rangle$$
 (9)

The wake production term appears as a horizontal average of the product of local deviations of Reynolds stresses and velocity gradients from their spatial-averaged values. This term produces turbulent kinetic

energy in the same way as the shear production term. The fifth term on the right in (9) represents a wake production (source) term, similar to the fourth term in (6).

Careful analysis of these expressions provides better insight into the turbulence structure and its generation mechanisms inflows through vegetation, and helps to clarify the ambiguity in the drag-related coefficients (previously used to model the drag-induced turbulence production). It is observed that two characteristic processes act as turbulent kinetic energy generators to transfer energy from larger scales (either mean flow or larger eddies) toward turbulent fluctuations in space or time at smaller scales: (a) the work of Reynolds and dispersive stresses against mean velocity gradients; and (b) the work of mean flow or large eddies against pressure differences due to the obstacles. Looking at (4) and at the first term on the right of (6), the action of mechanism (a) may be subdivided as

$$\langle \bar{u}_i \bar{u}_i \rangle \frac{\partial \langle \bar{u}_j \rangle}{\partial x_i} \tag{9a}$$

Which is the same as the first term on the right of (8) contributes to the generation of fluctuations in time, and

$$\langle \bar{u}_i' \bar{u}_i' \rangle \frac{\partial \langle \bar{u}_j \rangle}{\partial x_i} \tag{9b}$$

which is equal to the first term on the right of (9) and generates spatial perturbations of time-averaged values. The work of the mean flow against pressure differences in space, mechanism (b), is a source term for the budget of spatial fluctuations of time-averaged velocities, where a shear generation-like term appears as a sink and transfers energy from space fluctuations toward small-scale fluctuations in time. There are two limiting cases worth analyzing. The first one, in the work of Raupach and Shaw (1982) concerns the case where the length scale of the canopy elements (and of their wakes, or in other words, the scale of the wake-generated turbulence) is much larger than the Kolmogorov micro scale,  $h$ , so that the viscous term in (9) becomes negligible. In this situation, if all the dispersive fluxes are considered to be a lower order of magnitude, then for steady advection-free conditions, (9) reduces to

$$-\langle \bar{u}_i' \bar{u}_j' \rangle \frac{\partial \bar{u}_i'}{\partial x_i} = \frac{1}{\rho} \langle \frac{\partial \bar{p}'}{\partial x_i} \rangle \tag{10}$$

which means that the work of the mean flow against pressure differences becomes equal to the wake production term for the turbulent fluctuations in time. The other limiting case occurs when the length scale of the canopy elements (the scale of the wake-generated turbulence) is much smaller than (or maybe even of the order of) the Kolmogorov micro scale. In this situation, most of the energy arising from the work of the mean flow against pressure forces is spent in the generation of spatial fluctuations, and therefore, is directly dissipated into heat. In steady advection free conditions (9)

$$-v \langle \bar{u}_i' \nabla^2 \bar{u}_i' \rangle = \frac{1}{\rho} \langle u_i \rangle \langle \frac{\partial \bar{p}'}{\partial x_i} \rangle \tag{11}$$

So that

$$-\langle \bar{u}_i' \bar{u}_j' \rangle \frac{\partial \bar{u}_i'}{\partial x_i} \approx 0 \tag{11a}$$

and there is a negligible contribution from the wakes to the spatial average of the turbulent fluctuations in time. The first of these two situations are commonly found in atmospheric flows; the second situation is more common in water flows with relatively low plant densities. This is reasonable, since the Kolmogorov micro scale is normally smaller in air than in water. The characteristic length scales of canopy elements in atmospheric flows are expected to be much larger than those found in water flows. The discussion, in the previous paragraphs, clarifies the problem concerning the different coefficients assigned to the wake generation terms in the conservation equations for  $k$  and  $\epsilon$  in different turbulence models. It becomes obvious that when numerically modeling the spatial average of the local, time averaged turbulent kinetic energy (or any  $\langle \bar{u}_i'^2 \rangle$  for that matter) in a flow with elements in the order of the Kolmogorov microscale, the wake-related source term in the energy equation becomes negligible. In other words, the drag-related weighting factors in the turbulent kinetic energy and in the dissipation, equations would be very close to zero. For the numerical computation of the total turbulent kinetic energy,  $\langle \bar{u}_i' \bar{u}_i' \rangle + \langle \bar{u}_i' \bar{u}_j' / 2 \rangle$ , these

coefficients are expected to be close to 1.0 and 1.33, respectively (Lopez and Garcia 1997).

### CONCLUSION

This paper reviewed some works related to vegetated open channel flow and the findings from this review suggests that there is need to improve the existing models for predicting both the optimum roughness and flow discharge respectively. A number of numerical, Mathematical and Analytical Simulation models were performed in order to test their ability to predict the flow field in the presence of vegetation. A comparison between experimental data and the results of these simulations clearly demonstrates that both models can fairly accurately reproduce the vertical profiles of velocity and shear stress within and above vegetation. Authors' (as in the case of Kothyari et al. 2009; Tanino and Nepf 2008; Nguyen, 2012; Ferreira et al. 2009; Ishikawa et al. 2000; James et al. 2004; Liu et al. 2008; Ishikawa et al. 2000 and Kothyari et al. 2009) makes use of vegetation coverage over the inclined riverbank which confirmed the increased in stream wise velocity in the main channel compared with the inclined bank surface. Velocity in the downstream direction decreased in the vicinity of riverbank/main channel interface and over the bank in all the configurations. Surprisingly, the rigid elements generated velocity and shear stress distribution almost similar to the stream bank supporting the previous findings of the Valyrakis et al. (2015). It can be concluded that more research is required using natural vegetation in order to overcome the shortfall of artificial vegetation.

### RECOMMENDATION

This study was conducted to improve the understanding of the hydrodynamics of open channel flows by evaluating the effects of vegetation on flow properties like velocity profiles, Reynolds shear stresses, and turbulent intensities e.t.c. These analysis and results can be further treated in order to raise comments on the morphological changes that can occur due to the sediment transport and thus propose stream restoration plans especially for flood control analysis. On the other hand, already available models can be altered to obtain the effects of changes on the proposed models. These changes can be variable

discharge, variable bank slopes and flexible vegetation above the inclined bank. Similar study can also simulate the super-critical flow conditions. By using the St. Venant equations in the simulations, unsteady flow conditions and variable bed morphology can be added to the future studies.

### REFERENCES

- [1] Aerle, J., & Järvelä, J. (2013). Flow resistance of emergent rigid and flexible floodplain vegetation. *Journal of Hydraulic Research*, 51(1), 33-45.
- [2] Afzalimehr, H., Moghbel, R., Gallichand, J., & Sui, J. (2011). Investigation of turbulence characteristics in channel with dense vegetation. *International Journal of Sediment Research*, 26(3), 269-282.
- [3] Augustijn, D.C.M, Huthoff, F., & Velzen, van E.H., 2008. Comparison of vegetation roughness descriptions. *River flow 2008; international conference on fluvial hydraulics*.
- [4] Baptist, M.J., Babovic, V., Rodrigues Uthurburu, J., Keijzer, M., Uittenbogaard, R.E., Verway, A., & Mynett, A.E., 2006. On inducing equations for vegetation resistance. *Journal of Hydraulic Research*, 45(4), 435-450.
- [5] Besserebrennikov, N.K., 1958. Some regulations of the movement of water in vegetated channels of drainage system canals. *Dokl. Akad. Nauk BSSR*, 11.
- [6] Borovkov, V.S. and Yurchuk, M., 1994. Hydraulic resistance of vegetated channels. *Hydrotechnical Construction*, 8, 28.
- [7] Bos, de W.P. and Bijkerk, V., 1963. Een nieuw monogram voor het berekenen van waterlopen. *Cultuurtechnisch Tijdschrift*, 4, 149-155.
- [8] Brown, G.O. (2002). The history of the Darcy-Weisbach equation for pipe flow resistance. *Environmental and water resources history*, 34-43.

- [9] Buckman, L. (2013). Hydrodynamics of partially vegetated channels: stem drag forces and application to an in-stream wetland concept for tropical, urban drainage systems. Delft (MSc thesis report).
- [10] Carollo, F., Ferro, V., & Termini, D. (2002). Flow velocity measurements in vegetated channels. *Journal of Hydraulic Engineering*, 128(7), 664-673.
- [11] Carollo, F.G., Ferro, V. and Termini, D., 2005. Flow resistance law in channels with flexible submerged vegetation. *Journal of Hydraulic research* 131, 554-564.
- [12] Chen, Y.-C., Kao, S.-P., Lin, J.-Y., & Yang, H.-C. (2009). Retardance coefficient of vegetated channels estimated by the Froude number. *Ecological Engineering*, 35(7), 1027-1035.
- [13] Chlebek, J. (2009). Modelling Of Simple Prismatic Channels With Varying Roughness Using The Skm And A Study Of Flows In Smooth Non-Prismatic Channels With Skewed Floodplains. Unpublished PhD Thesis, The University of Birmingham
- [14] David, L. (2008). Flow through Rigid Vegetation Hydrodynamics. Thesis of Master of Science, Virginia Polytechnic Institute and State University.
- [15] Dijkstra, J.T. & Uittenbogaard, R.E., 2006. Modelling hydrodynamics in flexible vegetation. *Physical Processes in Natural Waters workshop*, Sept 4-7, Lancaster, England.
- [16] Dunn, C., Lopez, F., and García, M., 1996. Mean flow and turbulence in a laboratory channel with simulated vegetation. *Hydraulic Engineering Series*. 51. University of Illinois at Urbana-Champaign, Urbana, Illinois.
- [17] El-Samman, T. A., Hosny M. M. and Ibrahim H. M. . (1999). Impact of Aquatic Weeds on Water Distribution Efficiency. The 2nd Inter-Regional Conference on Environment - Water Engineering Technologies for Sustainable Land use and Water Management. Switzerland.
- [18] Einstein, H.A. and Banks, R.B., 1950. Fluid resistance of composite roughness. *American Geophysical Union*, 3, 603-634.
- [19] Fathi-Maghadam and M., Kouwen, N., 1997. Nonrigid, nonsubmerged, vegetative roughness on floodplains. *Journal of hydraulic engineering*, 123, 51-57.
- [20] Fischenich, C., 2000. Resistance due to vegetation. EMRRP Technical Notes, ERDC TNEMRRP- SR-07, Us Army Engineer Research and Development Center, Vicksburg, MS.
- [21] Freeman, F.E., Rahmeyer, W.J., and Copeland, R.R., 2000. Determination of resistance due to shrubs and woody vegetation. Technical report, U.S. Army Engineer Research and Development Center, Vicksbur, MS.
- [22] Ferreira, R. M. L., Ricardo, A. M., and Franca, M. J. (2009). Discussion of "Laboratory Investigation of Mean Drag in a Random Array of Rigid Emergent Cylinders" by Yukie Tanino and Heidi M. Nepf. *Journal of Hydraulic Engineering ASCE*, 135(8), 690 - 693.
- [23] Guscio, F. J., Bartley, T. R., & Beck, A. N. (1965). Water resources problems generated by obnoxious plants. *Proceedings of the American Society of Civil Engineers, Journal of the Waterways and Harbours Division*, 10, 47-60.
- [24] Ghisalberi, M. and Nepf, H., 2004. The limited growth of vegetated shear layers. *Water Resources Research*. 40, W07502.
- [25] Ghisalberti, M. and Nepf, H., 2006. The structure of the shear layer over rigid and flexible canopies. *Environmental Fluid Mechanics*, 6, 277-301. Gourlay, M.R., 1970. Discussion of 'Flow retardance in vegetated channels' by N. Kouwen, T.E. Unny and H.M. Hill. *Journal of Irrigation Drainage Engineering*. 96, 351-357.

- [26] Green, J.C., 2005. Modelling flow resistance in vegetated streams: review and development of new theory. *Hydrological processes*, 19, 1245-1259. HEC-RAS User Manual Version 4.0, 2008. US Army Corps Of Engineers.
- [27] Gwinn, W., & Ree, W. (1980). Maintenance effects on the hydraulic properties of a vegetation-lined channel. *Transactions of the ASAE*, 23(3), 636-642.
- [28] Hamimed, A., Nehal, L. M., Benslimane, M., & Khaldi, A. (2013). Contribution to the Study of the Flow Resistance in a Flume with Artificial Emergent Vegetation. *Larhyss Journal*, 15(2013), 9.
- [29] Hassan, I. M. (2010). Flow Characteristics of Partially Vegetated Trapezoidal Channel Cross-Section with Flexible Vegetation. Fourteenth International Water Technology Conference, IWTC 14 2010. . Cairo, Egypt.
- [30] Helmiö, T. (2005). Unsteady 1D flow model of a river with partly vegetated floodplains—application to the Rhine River. *Environmental Modelling & Software*, 20(3), 361-375.
- [31] Hoffmann, M.R., 2004. Application of a simple space-time averaged porous media model to flow in densely vegetated channel. *Journal of porous media*, 7(3), 183-191.
- [32] Hong, H.T.M., 1995. Hydraulic Resistance of Flexible Roughness, M.Sc. Thesis HH237, IHE Delft.
- [33] Huthoff, F., 2007. Modelling hydraulic resistance of floodplain vegetation, PhD Thesis, Department of Water Engineering, University Twente.
- [34] Huthoff, F. (2013). Evaluation of a Simple Hydraulic Resistance Model Using Flow Measurements Collected in Vegetated Waterways. *Open Journal of Modern Hydrology*, 03(01), 28-37. doi: 10.4236/ojmh.2013.31005
- [35] Ikeda, S., & Kanazawa, M. (1996). Three-dimensional organized vortices above flexible water plants. *Journal of Hydraulic Engineering*, 122(11), 634-640.
- [36] Järvelä, J., 2003. Flow resistance of flexible and stiff vegetation: a flume study with natural plants. *Journal of Hydrology* 269, 44-54.
- [37] Klopstra, D., Barneveld, H.J., Van Noortwijk, J.M. and Van Velzen, E.H., 1997. Analytical model for hydraulic roughness of submerged vegetation. *Proceedings of the 27th IAHR Congress theme A Managing Water: Coping with Scarcity and Abundance*, San Fransisco,775-780.
- [38] Kouwen, N., Unny, T.E., and Hill, H.M., 1969. Flow retardance in vegetated channels. *Journal of Irrigation Drainage Engineering*, 95(2), 329-344.
- [39] Kouwen, N. and Unny, T. E., 1973. Flexible roughness in open channels. *Jouarnal of the Hydraulics Division, ASCE, HY5*, 713-728.
- [40] Kouwen , N., 1989. Field estimation of the biomechanical properties of grass. *Journal of Hydraulic research*, 5, 559-568.
- [41] Knighton, D. (1998). *Fluvial forms & processes, a new perspective*. Oxford University Press Inc.
- [42] Kutija, V. and Hong, H.T.M., 1996. A numerical model for assessing the additional resistance to flow introduced by flexible vegetation. *Journal of Hydraulic Research*, 1, 99-114.
- [43] López, F., and García, M.H., 2001. Mean flow and turbulence structure of open channel flow through non-emergent vegetation. *Journal of Hydraulic Engineering* 127, 392-402.
- [44] Ludov, V.A., 1976. Determination of the rational width of the strip and discharge of the irrigation stream during strip-liman irrigation. *Inform. Listok Krasnoyarskogo TsNTI*, 245.

- [45] Manz, D.H. and Westhoff, D.R. 1988. Numerical analysis of the effects of aquatic weeds on the performance of irrigation conveyance systems. *Can. J. Civil Engineering*, 15, 1-13.
- [46] Mitchell, D. S. (1974). *The Effects of Excessive Aquatic Plant Populations*, In: Mitchell, D. S. (Ed.) *Aquatic Vegetation and its Control*. Paris: UNESCO.
- [47] Poggi, D. and Katul, G.G., 2008. Hydraulic resistance of submerged rigid vegetation derived from first order closure models. *River flow 2008; international conference on fluvial hydraulics*
- [48] Ree, W.O., and Crow, F.R., 1977. Friction factors for vegetated waterways of small slope. Technical Report Publication S-151, US Department of Agriculture, Agricultural Research Service.
- [49] Rowinski, P.M. and Kubrak, J., 2002. A mixing-length model for predicting vertical velocity distribution in flows through emergent vegetation. *Hydrological Sciences-Journal des Sciences Hydroliques*, 47, 893-904.
- [50] Rowinski, P.M., Kubrak, E. and Kubrak, J. (n.d.) Vertical velocity distribution in flows through stiff, emergent and flexible submerged vegetation in open channels.
- [51] Wilson, C.A.M.E.; Stoesser, T.; Bates, P.D.; Pinzen, A.B (2003). Open channel flow through different forms of submerged flexible vegetation. *Journal of Hydraulic Engineering*. 2003, 129, 847–853.
- [52] Wilson, C. A. M. E., Yagci, O., Rauch, H. P., & Olsen, N. R. B. (2006). 3D numerical modelling of a willow vegetated river/floodplain system. *Journal of Hydrology*, 327(1-2), 13-21.